Yamashita et al., http://www.jcb.org/cgi/content/full/jcb.201106141/DC1

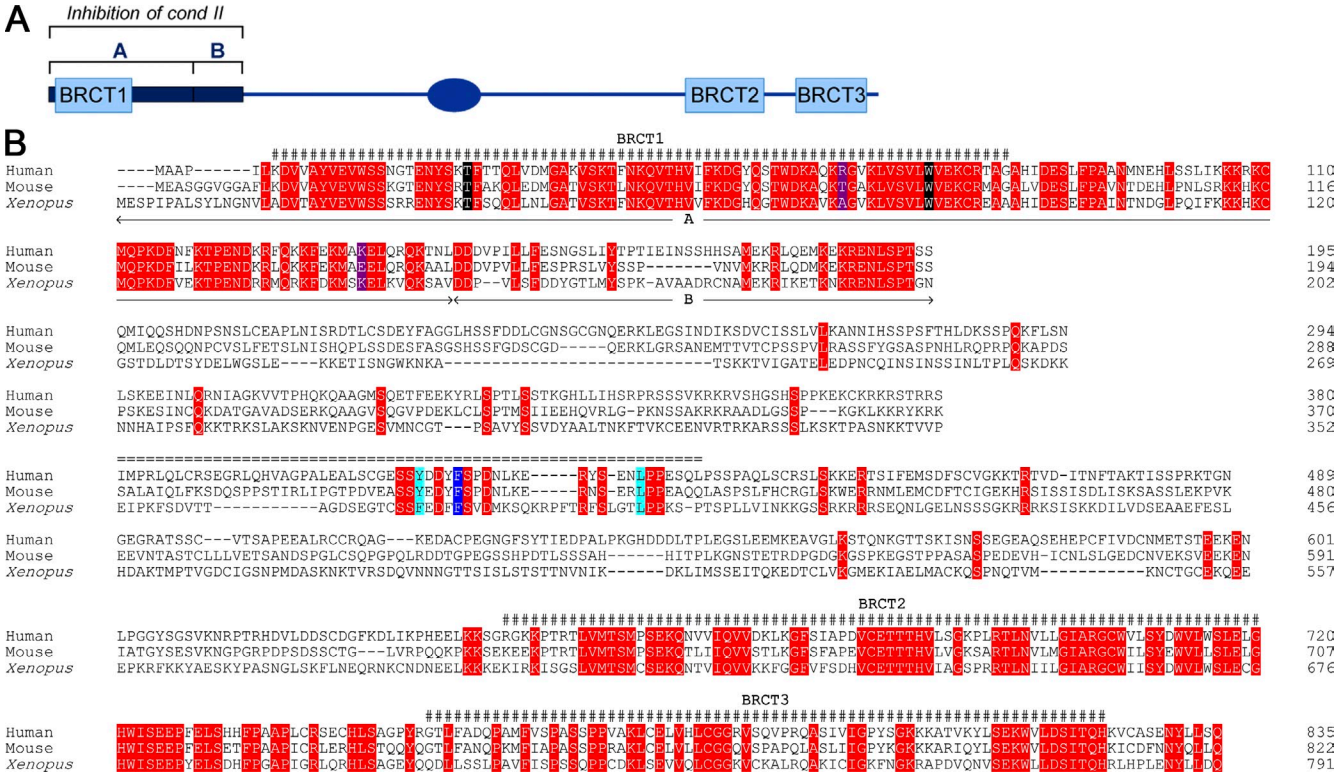

Figure S1. **Primary structures of vertebrate MCPH1.** (A) Schematic representation of the primary structure of MCPH1. (B) Sequence alignment of MCPH1 from three vertebrate species (*Homo sapiens* [human], *Mus musculus* [mouse], and *Xenopus*). Identical residues among the three polypeptides are highlighted in red, and three BRCT domains are indicated by #. Sequences outside of the BRCT domains are highly divergent among the three vertebrate species, indicating that MCPH1 is a rapidly evolving protein. Residues whose mutations cause primary microcephaly (T27 and W75 in humans) are highlighted in black. Two N-terminal subdomains (A, amino acids 1–145; B, amino acids 146–195 in humans) tested in Fig. 5 (A and B) are also indicated. Residues substituted in Fig. 5 (B and C) are highlighted in purple (R66 and K136 in humans; T72 and E142 in mice). The central domain interacting with condensin (cond) II (amino acids 381–435 in humans) is indicated by an equals sign, and residues substituted in Figs. 6 and S4 E are highlighted in light blue (Y412 and L429 in humans) and deep blue (F416 in humans).

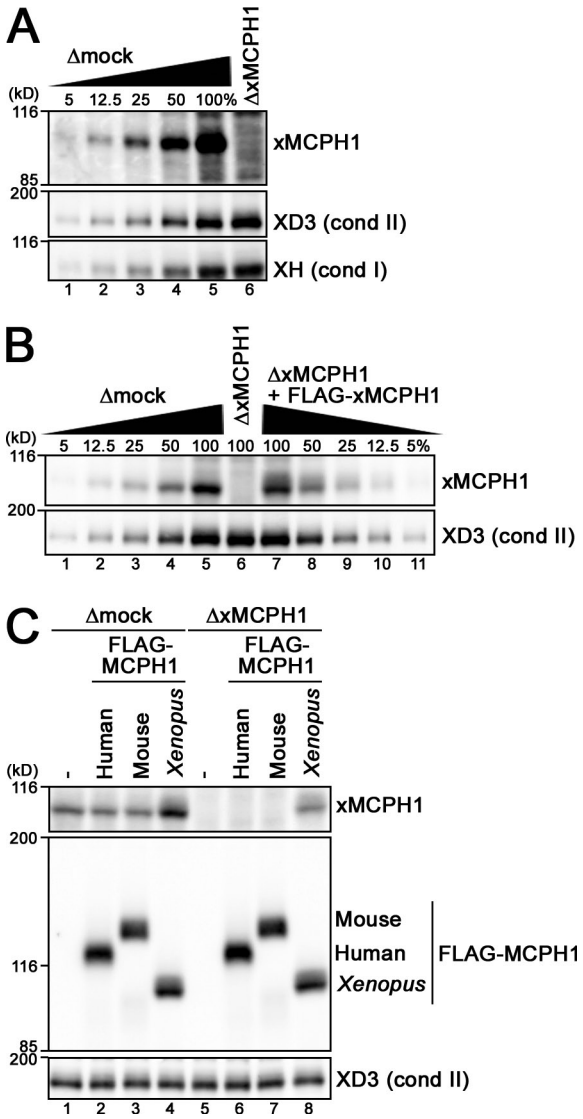

Figure S2. **Amounts of exogenously added MCPH1 proteins are comparable with that of endogenous xMCPH1.** (A) An egg extract was immunodepleted with control IgG (Δmock; lanes 1–5) or an antibody against xMCPH1 (ΔxMCPH1; lane 6). To estimate the efficiency of depletion, aliquots of each extract, along with decreasing amounts of the Δmock extract, were analyzed by immunoblotting with antibodies against xMCPH1, XCAP-D3 (XD3), and XCAP-H (XH). Note that >95% of endogenous xMCPH1 were depleted from the ΔxMCPH1 extract. (B) The Δmock extract was mixed with 0.1 vol reticulocyte lysate containing no xMCPH1 (lanes 1–5), whereas the ΔxMCPH1 extract was mixed with 0.1 vol lysate containing no xMCPH1 (lane 6) or the standard amount of xMCPH1 (lanes 7–11). Each mixture was incubated for 120 min. Decreasing amounts of aliquots from each mixture were analyzed by immunoblotting with the indicated antibodies. The results indicated that the standard amount of FLAG-xMCPH1 added exogenously was comparable with that of xMCPH1 present in the egg extract. (C) The Δmock or the ΔxMCPH1 extract was mixed with 0.1 vol lysate containing no MCPH1 (lanes 1 and 5) or a lysate containing the standard amount of hMCPH1 (lanes 2 and 6), mMCPH1 (lanes 3 and 7), or xMCPH1 (lanes 4 and 8). Each mixture was incubated for 120 min, and then, aliquots from each mixture were analyzed by immunoblotting with the indicated antibodies. The results showed that the standard amounts of FLAG-hMCPH1, -mMCPH1, and -xMCPH1 added exogenously were comparable with that of xMCPH1 present in the egg extract. The FLAG data are derived from a different membrane than the xMCPH1 and XD3 data. cond, condensin.

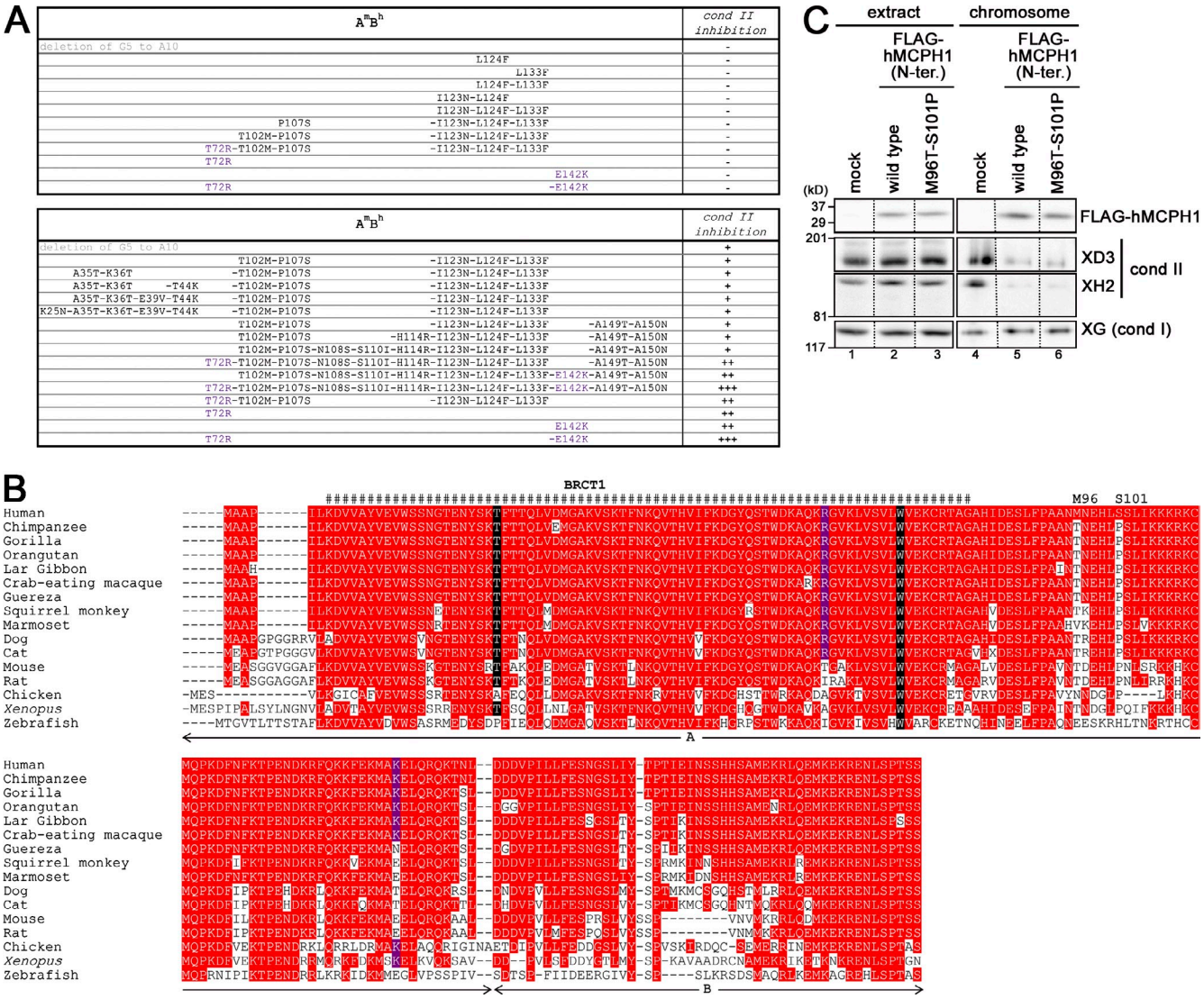

Figure S3. **Mouse to human and human to mouse conversions in the cell-free assay.** (A) Mouse to human conversion. Shown here is a list of mutation sites used in our attempt to convert the mouse sequence into a form that is competent to inhibit condensin II in the cell-free assay. Note that many of the mutations listed here, either individually or in combinations, hardly increased the ability of mMCPH1 (A^mB^m) to inhibit condensin II loading as judged by the cell-free assay (indicated by minus signs). Only the specific combination of the three substitutions, namely, T72R, E142K, and B^m>B^h (A^mB^h), was able to confer a humanlike activity on the mouse sequence as shown in Fig. 5 (A and B; indicated by triple plus signs). Mutations displaying intermediate activities are indicated by single or double plus signs. (B) Sequence alignment of MCPH1 from 16 vertebrate species (*Homo sapiens* [human], *Pan troglodytes* [chimpanzee, NP_001009010.1], *Gorilla gorilla* [gorilla, P61591.1], *Pongo pygmaeus* [orangutan, P61594.1], *Hylobates lar* [lar gibbon, P61592.1], *Macaca fascicularis* [crab-eating macaque, Q5IFK1.1], *Colobus guereza* [guereza, P61590.1], *Saimiri boliviensis* [squirrel monkey, AAS92244.1], *Callithrix jacchus* [marmoset, XP_002756799.1], *Canis lupus familiaris* [dog, NP_001003366.1], *Felis catus* [cat, NP_001009348.1], *Mus musculus* [mouse], *Rattus norvegicus* [rat, XP_225006.5], *Gallus gallus* [chicken, NP_001098789.1], *Xenopus laevis* [*Xenopus*], and *Danio rerio* [zebrafish, AAH91882.1]; accession numbers were obtained from the NCBI Protein database). Identical residues with hMCPH1 are highlighted in red, and the BRCT1 domain is indicated by #. Residues whose mutations cause primary microcephaly (T27 and W75 in humans) are highlighted in black. Two N-terminal subdomains (A, amino acids 1–145; B, amino acids 146–195 in humans) are also indicated. Residues substituted in Fig. 5 (B and C) are highlighted in purple (R66 and K136 in humans; T72 and E142 in mice). Amino acid residues unique to humans (M96 and S101) are also indicated. (C) Wild-type and mutant (M96T-S101P) forms of the N-terminal (N-ter.) domain (amino acids 1–195) of hMCPH1 were subjected to the cell-free assay. Chromosome fractions and aliquots of the extracts were analyzed by immunoblotting. The dotted lines indicate where intervening lanes were removed for presentation purposes. Note that the M96T-S101P mutant retained the same level of condensin (cond) II inhibitory activity as wild-type hMCPH1. XG, XCAP-G; XH2, XCAP-H2.

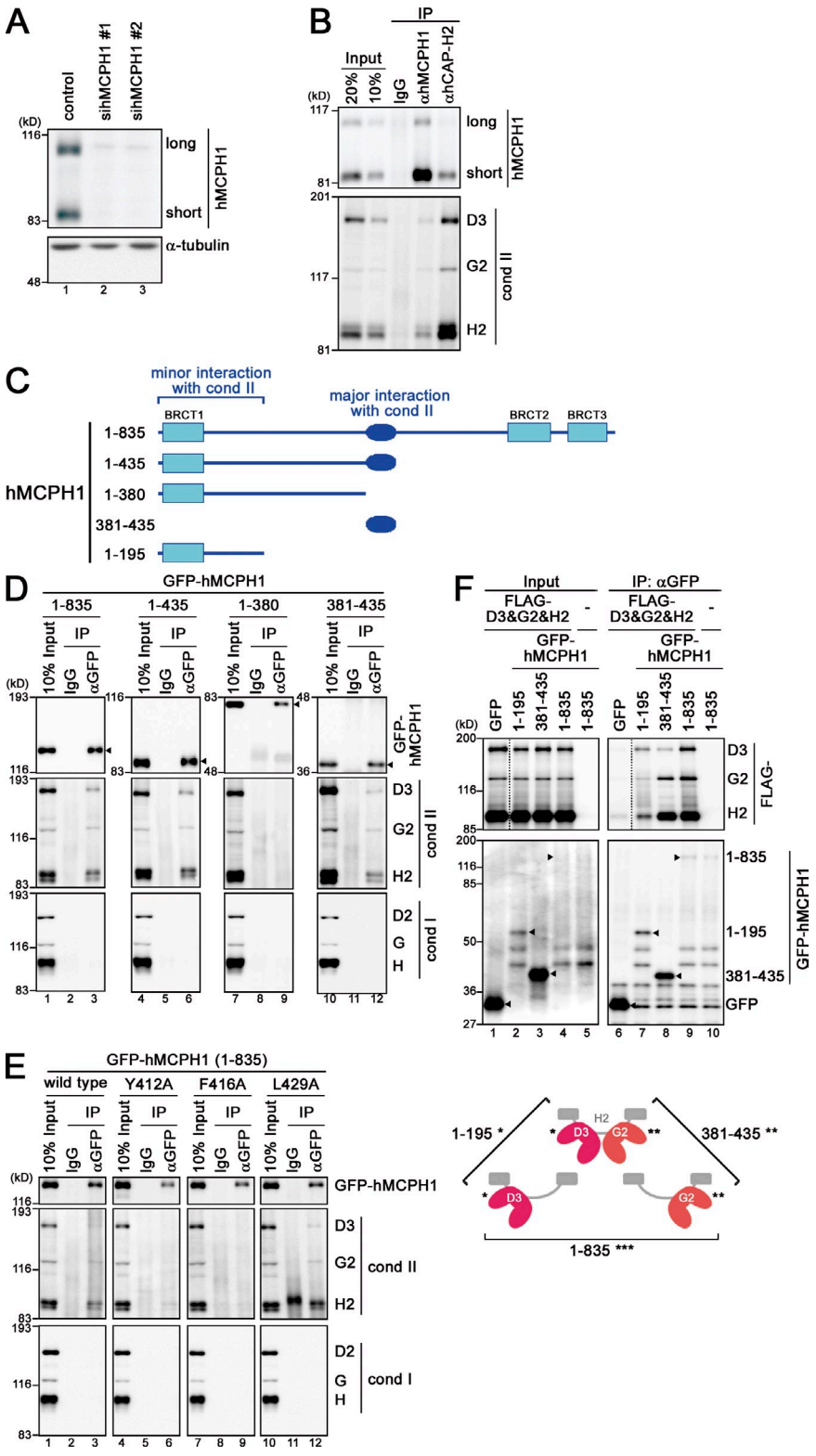

Figure S4. **Additional evidence for physical interactions between hMCPH1 and condensin II.** (A) HeLa cells were transfected with two different siRNAs targeted for hMCPH1 (lanes 2 and 3) or without siRNAs (control; lane 1) and analyzed for protein levels by immunoblotting with anti-hMCPH1 and anti–α-tubulin. α-Tubulin was used as a loading control. A pair of bands with an apparent molecular mass of ~110 kD (long) and ~85 kD (short) was detected in the control sample, whereas the level of both bands was specifically reduced upon treatment with hMCPH1 siRNAs. We have evidence that the short form is a naturally truncated form of full-length hMCPH1 (i.e., the long form; not depicted). (B) HeLa nuclear extracts were subjected to immunoprecipitation (IP) with control IgG (lane 3), anti-hMCPH1 (lane 4), or anti–hCAP-H2 (lane 5). The precipitates, along with 20 and 10% of the input fraction (lanes 1 and 2), were analyzed by immunoblotting with antibodies against hMCPH1, human CAP-D3 (D3), CAP-G2 (G2), and CAP-H2 (H2). The hMCPH1 data are derived from a different membrane than the condensin (cond) II data. (C) Schematic representation of hMCPH1 constructs used in D and F. (D and E) 293T cells were transfected with a plasmid expressing GFP-tagged hMCPH1. Cell lysates were prepared 24 h after transfection and subjected to immunoprecipitation with anti-GFP or control rabbit IgG. The precipitates, along with 10% of the input fractions, were analyzed by immunoblotting with antibodies against GFP, human CAP-D3, CAP-G2, CAP-H2, CAP-D2 (D2), CAP-G (G), and CAP-H (H). In D, the condensin I data are derived from a different membrane than the GFP and condensin II data for the left three datasets, whereas the GFP data are derived from a different membrane than the condensin I and II data for the rightmost dataset. In E, the condensin II data are derived from a different membrane than the GFP and condensin I data. The arrowheads indicate the positions of GFP-hMCPH1. An N-terminal half (amino acids 1–435) and an isolated central domain (amino acids 381–435) of hMCPH1, but not a shorter form (amino acids 1–380), coprecipitated condensin II as efficiently as full-length hMCPH1 did (D). This result indicated that the central domain (amino acids 381–435) is primarily responsible for hMCPH1's interaction with condensin II in this assay. A similar, if not identical, result had been reported previously by Wood et al. (2008). To further substantiate the specific interaction between the central domain and condensin II, site-directed mutagenesis was then performed. We focused on three conserved hydrophobic amino acid residues (Y412, F416, and L429) and created their alanine substitution mutants (Y412A, F416A, and L429A; Fig. S1). We found that two out of the three mutations (Y412A and F416A) abolished hMCPH1's ability to interact with condensin II (E). In the experiments shown in Figs. 6 and 7, we used the F416A mutant as a representative one. (F) FLAG-tagged non-SMC subunits (CAP-D3, -G2, and -H2) of human condensin II were translated individually in reticulocyte lysates, pooled, and then further incubated with another lysate containing GFP-tagged hMCPH1 (amino acids 1–195, 381–435, or 1–835). The mixtures were subjected to immunoprecipitation with anti-GFP, and the immunoprecipitates (lanes 6–10) and aliquots of the mixtures (lanes 1–5) were analyzed by immunoblotting with anti-FLAG and anti-GFP. The dotted lines indicate where intervening lanes were removed for presentation purposes. The FLAG data are derived from a different membrane than the GFP data. The arrowheads indicate the positions of GFP fusion proteins. The cartoons depict the D3-G2-H2 trimer and its subassemblies (i.e., dimers) that are formed in the pooled lysates (Onn et al., 2007). The N-terminal domain (amino acids 1–195) of hMCPH1 coprecipitated the D3-H2 dimer as well as the trimer, supporting the idea that its major binding partner is the D3 subunit (indicated by a single asterisk). On the other hand, the central domain (amino acids 381–435) coprecipitated the G2-H2 dimer and the trimer, supporting the idea that its major binding partner is the G2 subunit (indicated by a double asterisk). Consistently, full-length hMCPH1 (amino acids 1–835) precipitated both dimers and the trimer (indicated by a triple asterisk).

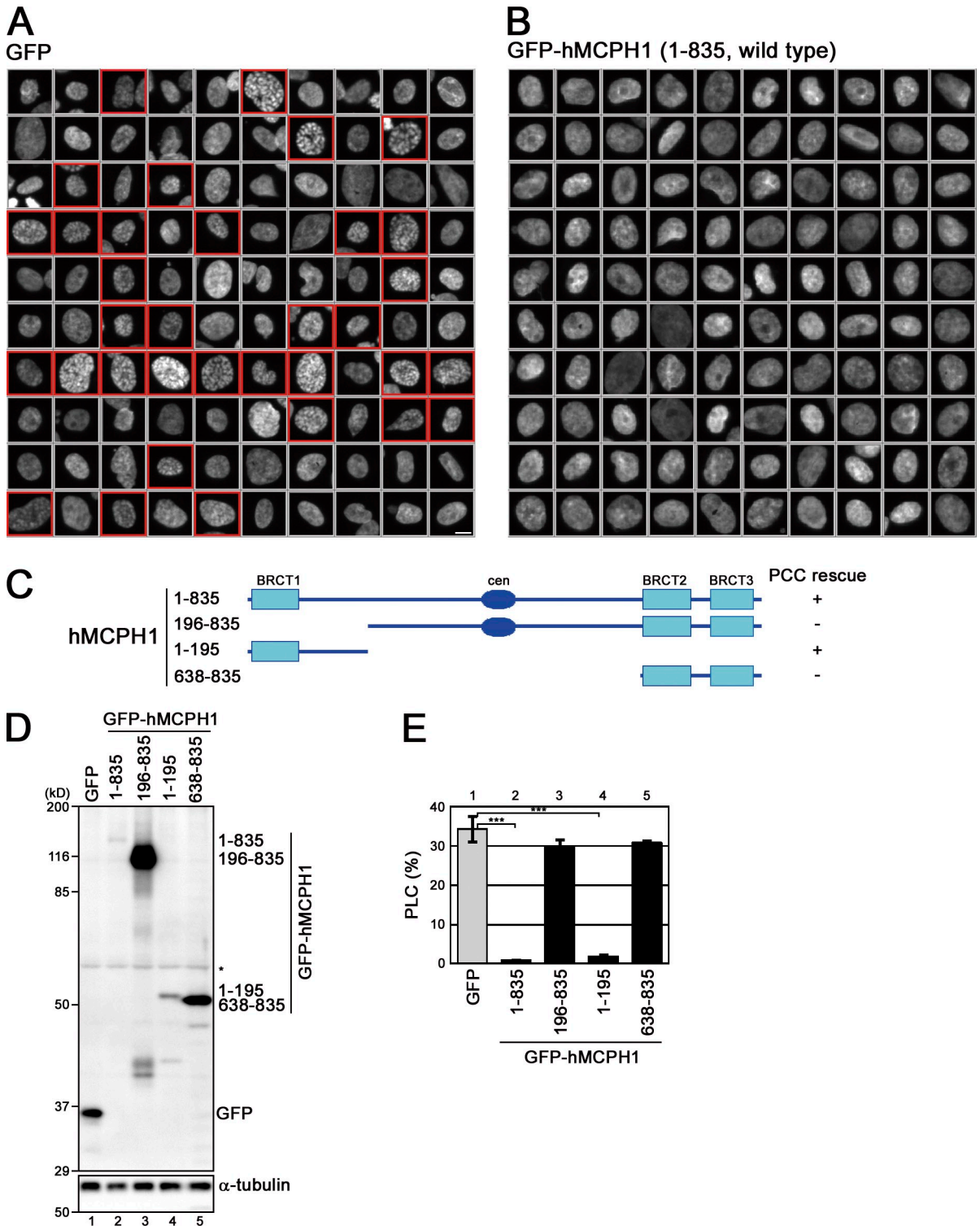

Figure S5. **The N-terminal domain of hMCPH1 is necessary and sufficient to rescue the PCC phenotype.** (A and B) GFP alone (A) or GFP-hMCPH1 (B) was expressed in patient cells, and GFP-positive populations were selected by using CELAVIEW. Shown here is a gallery of DAPI-stained images prepared from the two groups. Although ~30% of cells in the first group (indicated by the red rectangles) displayed a prophaselike morphology (A), virtually none of the cells in the second group displayed such a morphology (B). Bar, 10 µm. (C) Schematic representation of deletion constructs of hMCPH1 used in this study. (D) MCPH1 patient cells were transduced with GFP-tagged, full-length, and three truncated versions of hMCPH1 by means of a lentivirus expression system (lanes 2–5). Cells transduced with GFP alone (lane 1) were used as negative control. Lysates were prepared from these cells and analyzed by immunoblotting with anti-GFP (top) and anti–α-tubulin (bottom). α-Tubulin was used as a loading control. The asterisk indicates nonspecific bands. (E) The cells described in D were fixed and stained with DAPI. The percentages of PLCs were scored and plotted (***, $P < 0.001$ between each pair; PLCs were scored from three independently prepared coverslips [$n = 3$]). It should be noted that no statistical differences were observed among GFP and the two truncated versions (amino acids 196–835 and 638–835) lacking the N-terminal domain. Error bars indicate means ± SD.

References

Onn, I., N. Aono, M. Hirano, and T. Hirano. 2007. Reconstitution and subunit geometry of human condensin complexes. *EMBO J.* 26:1024–1034. http://dx.doi.org/10.1038/sj.emboj.7601562

Wood, J.L., Y. Liang, K. Li, and J. Chen. 2008. Microcephalin/MCPH1 associates with the Condensin II complex to function in homologous recombination repair. *J. Biol. Chem.* 283:29586–29592. http://dx.doi.org/10.1074/jbc.M804080200